Biodesign

pISSN 2288-6982 | eISSN 2288-7105

CRYSTALLIZATION P 44-48

Purification, crystallization, and preliminary X-ray crystallographic analysis of VV2_1132, a LysR-type transcriptional regulator from *Vibrio vulnificus*

Yongdae Jang[1], Garam Choi[1,2], Inseong Jo[1], Sang Ho Choi[1,2] and Nam-Chul Ha[1,*]

[1]Department of Agricultural Biotechnology, Research Institute for Agriculture and Life Sciences, Seoul National University, Seoul 08826, Republic of Korea, [2]National Research Laboratory of Molecular Microbiology and Toxicology.

*Correspondence: hanc210@snu.ac.kr

LysR-type transcriptional regulators (LTTRs) belong to the largest family of transcriptional regulators in prokaryotes. However, the crystal structures of only a few full-length LTTRs have been determined. LTTR HypT (also known as YjiE or QseD) from *Escherichia coli* specifically senses hypochlorite to protect oxidation damage by hypochlorite generated by the host immune system. In the genome of the highly virulent bacteria, *Vibrio vulnificus*, VV2_1132 showed the highest sequence similarity to *E. coli* HypT. In this study, we overexpressed full-length VV2_1132 in an *E. coli* expression system and crystallized the protein. The crystal diffracted X-rays to 2.2 Å resolution and belonged to the orthogonal space group $P2_12_12$, with unit cell parameters a = 57.8, b = 113.5, and c = 220.7 Å. Cell content analysis predicted that the asymmetric unit may contain four molecules of VV2_1132. For the case of four molecules in the asymmetric unit, the Matthews coefficient was 2.70 Å^3/Da with a solvent content of 54.5%. We are currently identifying the crystal structure of VV2_1132 using anomalous signals from selenomethione-substituted crystals. This crystal structure will help elucidate the function and action mechanism of VV2_1132, which may be involved in the pathogenesis of *V. vulnificus*.

INTRODUCTION

The LysR-type transcriptional regulator (LTTR) family is the largest transcriptional regulator family in prokaryotes. LTTRs regulate diverse biological functions including virulence, metabolism, quorum sensing, and motility. LTTRs have the conserved structural architecture of an N-terminal DNA binding domain (DBD) and a C-terminal regulatory domain (RD) (Maddocks and Oyston, 2008). Crystal structures of LTTRs have revealed that the RD adopts an α/β Rossmann fold to recognize cognate ligands or stimuli, while the DBD adopts a helix-turn-helix motif for DNA binding to regulate transcription (Choi et al., 2001; Jo et al., 2015; Maddocks and Oyston, 2008). Most LTTRs assemble into homotetramers with characteristic asymmetric conformations using two dimeric interfaces on the DBD and RD. OxyR is one of the most well characterized LTTR (Jo et al., 2015). The ligand hydrogen peroxide is bound in a small pocket in the RD dimer of OxyR, mediating a disulfide bond within the RD that results in a large conformational change in the RD dimers. This conformational change in the RD domains results in motion of the DBDs, triggering them to bind DNA (Jo et al., 2015). Numerous crystal structures of individual DBD or RD domains of several LTTRs have been reported. However, only a few crystal structures of the entire LTTR protein have been determined, presumably because of the difficulty in obtaining the full-length proteins or crystals (Das et al., 2015; Jo et al., 2015; Taylor et al., 2012).

In *Escherichia coli*, YjiE (or QseD) was first characterized as a LysR-type transcriptional regulator involved in quorum sensing and cell motility. Knock-out of *yjiE* increased motility in *E. coli* K-12 strain and altered Type 3 secretion, which is involved in quorum sensing in enterohemorrhagic *E. coli* (Habdas et al., 2010). YjiE was renamed HypT (hypochlorite-responsive transcription factor) in recent studies because it specifically confers hypochlorite resistance to *E. coli* (Drazic et al., 2014; Gebendorfer et al., 2012). YjiE was described as being able to sense HOCl by oxidation of three methionine and cysteine residues (Drazic et al., 2014; Drazic et al., 2013). However, the molecular mechanism and oligomerization state of the functional proteins remain unknown because of a paucity of crystal structures.

Vibrio vulnificus is a Gram-negative bacteria with a curved rod shape. This bacterium is an extremely virulent foodborne pathogen and can cause fatal septicemia in people with compromised immune systems (Jones and Oliver, 2009). Host innate immune systems produce diverse reactive oxygen species (ROS), such as hydrogen peroxide and hypochlorite (HOCl), to eliminate invading bacteria (Vatansever et al., 2013). In particular, neutrophils and certain types of epithelial cells produce hypochlorite (HOCl). *V. vulnificus* is equipped with elaborate

defense mechanisms to neutralize diverse types of host-generated ROS (Jones and Oliver, 2009). *V. vulnificus* has been shown to be resistant to peroxide stress. To sense peroxides, this bacterial species has two LysR-type transcriptional regulators, OxyR1 and OxyR2, which have different sensitivities to hydrogen peroxide (Kim et al., 2014).

To determine the HOCl resistance mechanism of *V. vulnificus*, we BLAST searched the *V. vulnificus* CMCP6 genome (accession number GCA_000039765.1) with *E. coli* YjiE or HypT sequences and identified a homologue, called VV2_1132 (accession number AAO08033.2). Sequence alignment of VV2_1132 with *E. coli* HypT and its homologue in *Salmonella enterica* serovar Typhimurium (S. Typhimurium) (accession number WP_000383509) revealed 30% and 29% sequence identities, respectively. Sequence similarities were higher for the N-terminal domain than the RD domain (Figure 1). We successfully overexpressed this protein in an *E. coli* expression system and obtained single crystals diffracting X-rays up to 2.2 Å resolution.

RESULTS AND DISCUSSION

Full-length VV2_1132 (residues 1-300) was successfully overexpressed in an *E. coli* expression system. The protein was purified to homogeneity by four subsequent steps consisting of affinity chromatography (Ni-NTA), cleavage of the hexahistidine tag by TEV protease treatment, anion exchange chromatography, and gel filtration chromatography. The final protein sample was concentrated to 9 mg/ml. The protein migrated as a single band on SDS-PAGE, with a molecular weight of ~34 kDa, and its purity was estimated to be >98% based on SDS–PAGE (Figure 2).

The protein was crystallized under several conditions from initial screening trials by the sitting drop vapor diffusion method. Crystals suitable for X-ray diffraction analysis were obtained in 0.1 M imidazole (pH 7.6), 0.9 M ammonium phosphate dibasic, 0.2 M NaBr, and 2 mM TCEP by the hanging drop vapor diffusion method at 14°C (Figure 3). The VV2_1132 protein crystals were flash-cooled in liquid nitrogen after being soaked in reservoir solution supplemented with 30% sorbitol. The diffraction dataset was collected using a highly brilliant undulator X-ray beam (beamline 5C in Pohang Accelerator Laboratory, Pohang, Republic of Korea) at a wavelength of 1.0082 Å. The best dataset was collected to 93.7% completeness with a resolution of 2.2 Å. The crystal lattice belonged to the primitive orthogonal space group, and analysis of diffraction along the *h*, *k*, and *l* axes revealed the space group of $P2_12_12$ with unit cell parameters of a = 57.8, b = 113.5, and c = 220.7 Å. Data collection statistics are given in Table 2.

Cell content analysis predicted that the number of molecules in the asymmetric unit was four or five (Table 2). Assuming five molecules in the asymmetric unit, the Matthews coefficient was calculated to be 2.16 Å^3/Da with a solvent content of 43.2%. For the case of four molecules in the asymmetric unit, the Matthews coefficient was 2.70 Å^3/Da with a solvent content of 54.5%

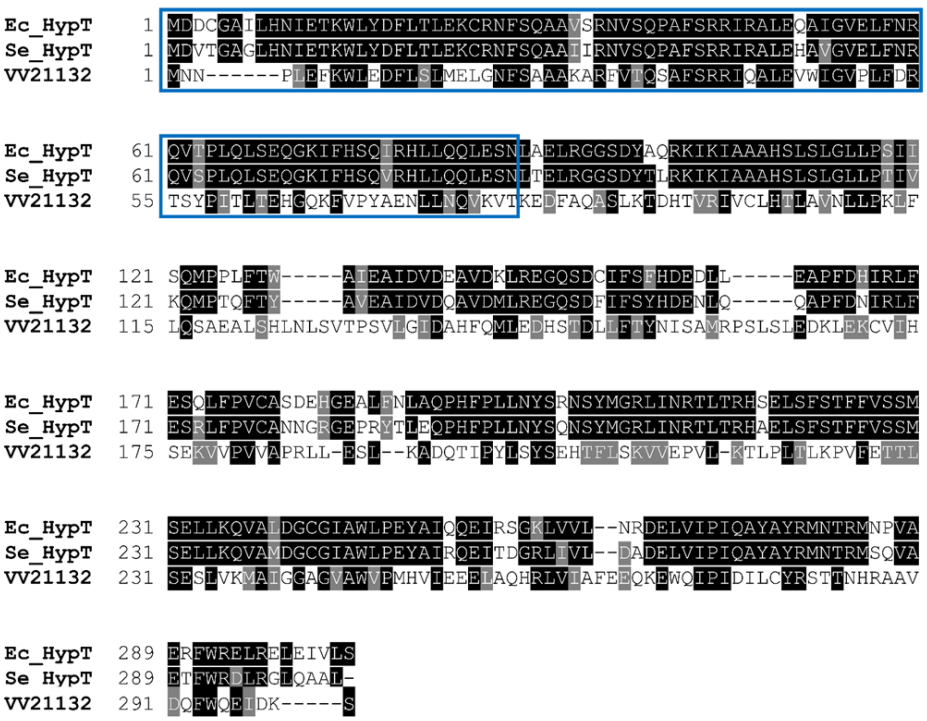

FIGURE 1 | Sequence alignment of VV2_1132 with *E. coli* and *S.* Typhimurium HypT. Blue boxes indicate the N-terminal DBD. Conserved residues are highlighted.

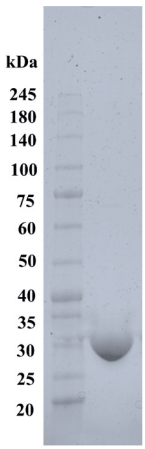

FIGURE 2 | The protein band on a 12-20% gradient SDS-polyacrylamide gel. The size marker is shown on the left.

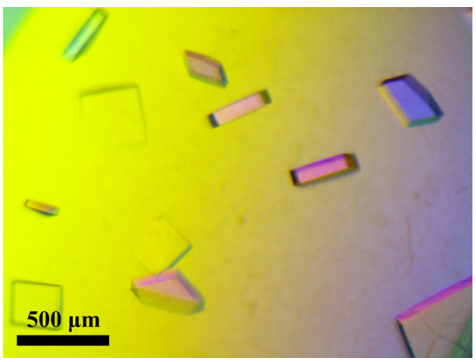

FIGURE 3 | Crystals of VV2_1132. The approximate dimensions of the crystals were 0.35 x 0.35 x 0.05 mm.

TABLE 1 | VV2_1132 production information

	VV2_1132
Source organism	*Vibrio vulnificus* CMCP6
DNA source	*Vibrio vulnificus* CMCP6 chromosomal DNA
Forward primer	GGTCCATGGCTATGAATAACCCACTAGAATTC
Reverse primer	GGTCCATGGCTATGAATAACCCACTAGAATTC
Cloning vector	pProEx-Hta
Expression vector	pProEx-Hta
Expression hose	*E. coli* BL21 (DE3)
Complete amino-acid sequence of the construct produced	GAMAMNNPLEFKWLEDFLSLMELGNFSAAAKAR FVTQSAFSRRIQALEVWIGVPLFDRTSYPITTEHGQ KFVPYAENLLNQVKVTKEDFAQASLKTDHTVRIV CLHTLAVNLLPKLFLQSAEALSHLNLSVTPSVLGI DAHFQMLEDHSTDLLFTYNISAMRPSLSLEDKLEK CVIHSEKVVPVVAPRLLESLKADQTIPYLSYSEHTF LSKVVEPVLKTLPLTLKPVFETTLSESLVKMAIGG AGVAWVPMHVIEEELAQHRLVIAFEEQKEWQIPID ILCYRSTTNHRAAVDQFWQEIDKS

(Matthews, 1968). A four-molecule structure in the asymmetric unit is more probable than five molecules because most LTTRs form a tetramer. To solve the structure of VV2_1132, molecular replacement was first attempted using the full-length structures of *P. aeruginosa* OxyR (PDB entry 4x6g ; 21% sequence identity) (Jo et al., 2015), *Vibrio cholerae* AphB (PDB entry 3sza ; 25% sequence identity) (Taylor et al., 2012), and *Neisseria meningitidis* CrgA (PDB entry 3hhg ; 21% sequence identity) (Das et al., 2015) as search models in the molecular replacement program *MOLREP* (Winn et al., 2011). Unfortunately, this method was not successful at finding correct solutions. We next attempted to obtain the experimental phases using the single-wavelength anomalous diffraction (SAD) approach. Because a high concentration of Br^- was used for crystallization as well as in the protein storage buffer, the crystals are likely to have bound Br-. However, even at a wavelength of a Br-absorption edge, namely 0.9801 Å, the anomalous signals were not sufficient to obtain the initial phases.

We are now attempting to apply the SAD approach to crystals labelled with selenium methionine. The crystal structure will help elucidate the function and action mechanisms of VV2_1132, thereby expanding our understanding of the structural diversity of LTTRs and potentially providing insight into the pathogenesis of *V. vulnificus*.

METHODS

Generation of the VV2_1132 construct

The gene coding for VV2_1132 was amplified from the *Vibrio vulnificus* CMCP6 genome by PCR. The primer sequences are described in Table 1. PCR products were digested with NcoI and XhoI and cloned into the pProEx-HTa vector (Invitrogen, USA), resulting in pProEX-HTa-VV2_1132 containing a hexahistidine tag and TEV cleavage site at the N-terminus of the protein to enable purification (Table 1).

Protein expression and purification of the VV_1132 protein

The recombinant plasmid pProEX-HTa-VV2_1132 was trans-formed into E. coli BL21 (DE3) cells. Cells were cultured in 1.6 L LB medium supplemented with 100 µg/mL ampicillin at 37°C until the OD_{600} reached 0.8. To induce expression of VV2_1132, cells were treated with IPTG (0.5 mM in the medium) and further cultured for 6-8 h at 30°C. Cells were harvested by centrifugation at 1,400xg for 10 min at 4°C. The bacterial pellet was resuspended in 50 ml of lysis buffer containing 20 mM Tris (pH 8.0), 150 mM NaCl, and 2 mM β-mercaptoethanol. Cells were disrupted by a continuous cell disruptor (Constant Systems, England), and the cell debris was removed by centrifugation at 20,000xg for 30 min at 4°C. The cell lysate (50 ml) containing VV2_1132 was incubated with 2 ml of Ni–NTA agarose resin (Qiagen, Germany) and rolled in a column for 30 min at 4°C. The resin was washed using 300 ml of lysis buffer

TABLE 2 | X-ray diffraction and cell content analysis

	VV2_1132	
Data collection		
Beam line	PAL 5C	
Wavelength (Å)	1.00820	
Rotation range per image (°)	1	
Total rotation range (°)	360	
Exposure time per image (s)	1	
Space group	$P2_12_12$	
Cell dimensions		
a, *b*, *c* (Å)	57.8, 113.5, 220.7	
α, β, γ (°)	90, 90, 90	
Resolution (Å)	50.0-2.20 (2.24-2.20)	
Total No. of reflections	2625351	
No. of unique reflections	75523	
R_{merge}	0.061 (0.494)	
High resolution shell CC1/2	0.219	
$I/\sigma I$	50.21 (12.6)	
Completeness (%)	93.7(83.8)	
Redundancy	8.3 (4.6)	
No. of molecules in asymmetric unit	4	5
V_M (Å^3/Da)	2.70	2.16
Solvent contents (%)	0.545	0.432

* Values in parentheses are for the highest resolution shell

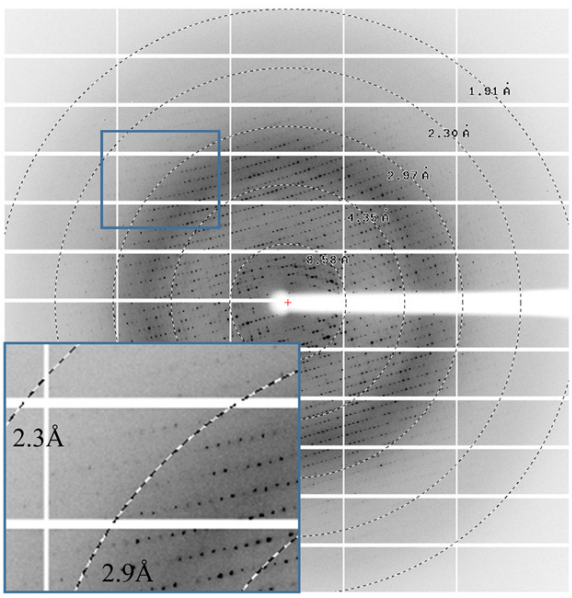

FIGURE 4 | **A representative diffraction image.** Resolution circles are indicated by the dotted lines. A rectangular area is enlarged in the left bottom corner.

supplemented with 20 mM imidazole (pH 8.0). The VV2_1132 protein was subsequently eluted with 30 ml of lysis buffer supplemented with 250 mM imidazole (pH 8.0). To cleave the hexahistidine tag from the protein, recombinant TEV protease (~1 mg) was added to the protein sample, and the sample was incubated overnight at 14°C (Tropea et al., 2009). The next day, the protein sample was diluted three-fold with 20 mM Tris (pH 8.0) buffer and then loaded onto a HiTrap Q anion exchange chromatographic column (GE Healthcare, USA). The protein was eluted from the column using a linear gradient of 0–1 M NaCl in 20 mM Tris (pH 8.0) buffer containing 2 mM β-mercaptoethanol. VV2_1132-containing fractions were pooled and concentrated to 5 ml using a Vivaspin centrifugal concentrator (30 kDa molecular-weight cutoff; Millipore, USA). The resulting protein sample was further purified using a gel filtration chromatographic column (HiLoad 16/60 Superdex 200; GE Healthcare), which was pre-equilibrated with 20 mM Tris buffer (pH 8.0) containing 150 mM NaBr and 2 mM β-mercaptoethanol. Fractions containing the VV2_1132 protein were pooled and concentrated to 9 mg/ml using the same concentrator and stored frozen at -80°C until use.

Crystallization

Initial crystallization of VV2_1132 was performed with commercially available screening solutions (MCSG, Anatrace) by the sitting-drop vapor-diffusion method at 14°C. In the initial crystallization screening experiments, 0.2 µl of protein solution (9 mg/ml) was mixed with 0.2 µl of reservoir solution and equilibrated against 60 µl of the reservoir solution. Small tetragonal or thick plate crystals were obtained in 0.1 M imidazole (pH 8.0), 1 M ammonium phosphate, 0.2 M NaCl, 2 mM Tris(2-carboxyethyl) phosphine (TCEP) at 14°C. Crystallization conditions were optimized using the hanging-drop diffusion method. Crystals suitable for further experiment grew from a solution containing 0.1 M imidazole (pH 7.6), 0.9 M ammonium phosphate dibasic, 0.2 M NaBr, and 2 mM TCEP at 14 °C. In the optimization experiments, 1 µl of the protein solution (9 mg/ml) was mixed with 1 µl of the reservoir solution and equilibrated against 500 µl of the reservoir solution. Thick plate-shaped crystals for data collection appeared in two days (Figure 3).

Data collection and processing

For data collection under cryogenic conditions, all crystals were transferred to 2 µl of cryo-protection buffer containing the reservoir solution supplemented with 30% sorbitol for 1 min and then flash-cooled in liquid nitrogen. X-ray datasets were collected at 1.0082 Å. Datasets were collected on a direct X-ray detector Pilatus 6M (Dectris, Switzerland) installed in beamline 5C of the Pohang Accelerator Laboratory, Republic of Korea. Complete diffraction datasets were subsequently processed, merged, and scaled with HKL-2000 (Otwinowski and Minor, 1997). Data collection statistics are provided in Table 2.

ACKNOWLEDGEMENTS

This research was supported by the R&D Convergence Center Support Program (to SHC and NCH) funded by the Ministry for Food, Agriculture, Forestry, and Fisheries, Republic of Korea, and NRF-2014R1A2A1A11050283 funded by the Ministry of Science, ITC, and Future Planning, Republic of Korea (to NCH). This study made use of beamline 5C at PLS (Pohang, Republic of Korea).

Original Submission: Feb 18, 2017
Revised Version Received: Feb 23, 2017
Accepted: Feb 23, 2017

AUTHOR INFORMATION

YJ, GC, and IJ performed the expreiments. YJ, GC, SHC, and NCH interpreted the results and wrote the manuscript.

REFERENCES

Choi, H., Kim, S., Mukhopadhyay, P., Cho, S., Woo, J., Storz, G., and Ryu, S.E. (2001). Structural basis of the redox switch in the OxyR transcription factor. *Cell* **105**, 103-113.

Das, N., Dai, J., Hung, I., Rajagopalan, M.R., Zhou, H.X., and Cross, T.A. (2015). Structure of CrgA, a cell division structural and regulatory protein from *Mycobacterium tuberculosis*, in lipid bilayers. *Proc Natl Acad Sci USA* **112**, E119-126.

Drazic, A., Gebendorfer, K.M., Mak, S., Steiner, A., Krause, M., Bepperling, A., and Winter, J. (2014). Tetramers are the activation-competent species of the HOCl-specific transcription factor HypT. *J Biol Chem* **289**, 977-986.

Drazic, A., Miura, H., Peschek, J., Le, Y., Bach, N.C., Kriehuber, T., and Winter, J. (2013). Methionine oxidation activates a transcription factor in response to oxidative stress. *Proc Natl Acad Sci USA* **110**, 9493-9498.

Gebendorfer, K.M., Drazic, A., Le, Y., Gundlach, J., Bepperling, A., Kastenmuller, A., Ganzinger, K.A., Braun, N., Franzmann, T.M., and Winter, J. (2012). Identification of a hypochlorite-specific transcription factor from *Escherichia coli*. *J Biol Chem* **287**, 6892-6903.

Habdas, B.J., Smart, J., Kaper, J.B., and Sperandio, V. (2010). The LysR-type transcriptional regulator QseD alters type three secretion in enterohemorrhagic *Escherichia coli* and motility in K-12 *Escherichia coli*. *J Bacteriol* **192**, 3699-3712.

Jo, I., Chung, I.Y., Bae, H.W., Kim, J.S., Song, S., Cho, Y.H., and Ha, N.C. (2015). Structural details of the OxyR peroxide-sensing mechanism. *Proc Natl Acad Sci USA* **112**, 6443-6448.

Jones, M.K., and Oliver, J.D. (2009). *Vibrio vulnificus*: disease and pathogenesis. *Infect Immun* **77**, 1723-1733.

Kim, S., Bang, Y.J., Kim, D., Lim, J.G., Oh, M.H., and Choi, S.H. (2014). Distinct characteristics of OxyR2, a new OxyR-type regulator, ensuring expression of Peroxiredoxin 2 detoxifying low levels of hydrogen peroxide in *Vibrio vulnificus*. *Mol Microbiol* **93**, 992-1009.

Maddocks, S.E., and Oyston, P.C. (2008). Structure and function of the LysR-type transcriptional regulator (LTTR) family proteins. *Microbiology* **154**, 3609-3623.

Matthews, B.W. (1968). Solvent content of protein crystals. *J Mol Biol* **33**, 491-497.

Otwinowski, Z., and Minor, W. (1997). Processing of X-ray diffraction data collected in oscillation mode. *Methods Enzymol* **276**, 307-326.

Taylor, J.L., De Silva, R.S., Kovacikova, G., Lin, W., Taylor, R.K., Skorupski, K., and Kull, F.J. (2012). The crystal structure of AphB, a virulence gene activator from *Vibrio cholerae*, reveals residues that influence its response to oxygen and pH. *Mol Microbiol* **83**, 457-470.

Tropea, J.E., Cherry, S., and Waugh, D.S. (2009). Expression and Purification of Soluble His6-Tagged TEV Protease. In High Throughput Protein Expression and Purification: Methods and Protocols, S.A. Doyle, ed. (Totowa, NJ: Humana Press), pp. 297-307.

Vatansever, F., de Melo, W.C., Avci, P., Vecchio, D., Sadasivam, M., Gupta, A., Chandran, R., Karimi, M., Parizotto, N.A., Yin, R., Tegos, G.P., Hamblin, M.R. (2013). Antimicrobial strategies centered around reactive oxygen species--bactericidal antibiotics, photodynamic therapy, and beyond. *FEMS Microbiol Rev* **37**, 955-989.

Winn, M.D., Ballard, C.C., Cowtan, K.D., Dodson, E.J., Emsley, P., Evans, P.R., Keegan, R.M., Krissinel, E.B., Leslie, A.G., McCoy, A., McNicholas, S.J., Murshudov, G.N., Pannu, N.S., Potterton, E.A., Powell, H.R., et al. (2011). Overview of the CCP4 suite and current developments. *Acta Crystallogr D Biol Crystallogr* **67**, 235-242.

